Plasmon modes of a massive Dirac plasma, and their superlattices

Rashi Sachdeva,[1,2] Anmol Thakur,[1] Giovanni Vignale,[3] and Amit Agarwal[1,*]
[1]*Department of Physics, Indian Institute of Technology Kanpur, Kanpur 208016, India*
[2]*Quantum Systems Unit, Okinawa Institute of Science and Technology Graduate University, Okinawa, Japan*
[3]*Department of Physics, University of Missouri, Columbia, Missouri 65211, USA*
(Received 26 February 2015; revised manuscript received 29 April 2015; published 19 May 2015)

We explore the collective density oscillations of a collection of charged massive Dirac particles, in one, two, and three dimensions, and their one-dimensional (1D) superlattice. We calculate the long-wavelength limit of the dynamical polarization function analytically, and use the random phase approximation to obtain the plasmon dispersion. The density dependence of the long-wavelength plasmon frequency in massive Dirac systems is found to be different compared to systems with parabolic and gapless Dirac dispersion. We also calculate the long-wavelength plasmon dispersion of a 1D metamaterial made from 1D and 2D massive Dirac plasma. Our analytical results will be useful for exploring the use of massive Dirac materials as electrostatically tunable plasmonic metamaterials and can be experimentally verified by infrared spectroscopy, as in the case of graphene [L. Ju *et al.*, Nat. Nanotechnol. **6**, 630 (2011)].

DOI: 10.1103/PhysRevB.91.205426 PACS number(s): 71.45.Gm, 73.21.−b, 77.22.Ch, 52.27.Ny

I. INTRODUCTION

The collective density oscillations of electrons liquids, i.e., plasmons, offer a powerful tool for exploring electron-electron interaction effects in various systems [1,2] and have also motivated several potential applications in optical metamaterials, nanophotonic lasers and amplifiers, biochemical sensing, and antennas transmitting and receiving light signals at the nanoscale [3,4]. The collective modes of ordinary (Schrödinger) electrons with parabolic dispersion [1,2,5] including spin-orbit coupling [6] and spin polarization [7] have been extensively studied in metals and doped semiconductors. Since the discovery of graphene, there has been huge interest in plasmons of Dirac materials and particularly in graphene [8–14], as it offers a tunable plasmon spectrum via electrostatic control of its carrier concentration and higher plasmon lifetimes due to high mobility.

There have been several studies on plasmons in gapless two-dimensional (2D) and three-dimensional (3D) Dirac systems in the context of graphene [15–19], topological insulators [20–22], Weyl semimetals [23], and in gapped 2D massive Dirac systems [24] in the context of buckled honeycomb structures such as silicene [25–27]. In addition to this, plasmons in periodic arrays of parabolic systems [28–31] and massless Dirac plasma layers [32–34] have also been investigated. A metamaterial made up of periodic graphene microribbon arrays was used in Ref. [8] to demonstrate tunable terahertz plasmon excitations in graphene. Comparatively, massive Dirac system in various dimensions and its multilayers/superlattice have been relatively less explored and consequently are the subject of this paper.

In this paper, we study the plasmon frequency and its density dependence for a massive Dirac plasma (MDP) interacting via the long-range Coulomb interaction, in one, two, and three dimensions. Additionally, we also calculate the plasmon dispersion for metamaterials made of 1D nanoribbons and 2D layers of MDP. The gapless Dirac systems were studied in Ref. [18], which serves as a check of all of our calculations in the limit of the vanishing band gap. We find that while the long-wavelength plasmon frequency in MDP is essentially quantum mechanical in nature, with $1/\sqrt{\hbar}$ appearing explicitly in the plasmon dispersion as in the case of gapless Dirac plasma (GDP), the scaling of the plasmon frequency with density is different for MDP, GDP, and parabolic systems. Note that in systems with nonrelativistic parabolic dispersion, the long-wavelength plasmon frequency is "classical" and quantum corrections (arising from the self-energy and vertex corrections in the polarization function) show up only in higher-order terms. The aim of this work is to illustrate the key differences between the density dependences of plasmon dispersions in one-, two-, and three-dimensional systems, which arise due to the relativistic (Dirac) or nonrelativistic (Schrödinger) nature of the electrons and due to the presence of a finite gap in MDP.

This article is organized as follows: In Sec. II, we introduce the random-phase approximation (RPA) "recipe" for calculating the plasmon frequency and explicitly calculate the long-wavelength limit of the dynamical polarization function for MDP, GDP, and parabolic dispersion systems. This allows us to obtain and discuss similarities and differences in the long-wavelength plasmon frequencies in Sec. III. Next we consider the plasmons arising in a periodic array of MDP nanoribbons and layers in Sec. IV and compare the results with GDP and parabolic dispersion systems. Finally, in Sec. V, we summarize our findings.

II. POLARIZATION FUNCTION

Within the RPA, the collective plasmon modes of an electron system emerge as poles of the density-density response functions (also called polarization function or the Lindhard function) and coincide with the zeros of the complex longitudinal "dielectric function" $\epsilon(q,\omega)$, i.e.,

$$\epsilon(q,\omega) = 1 - v_q \Pi(q,\omega) = 0, \tag{1}$$

where v_q is the Fourier transform of the Coulomb interaction and Π is the total noninteracting polarizability of the system.

*amitag@iitk.ac.in

The Fourier transform of the Coulomb interaction $v(r) = e^2/(\kappa r)$, in the appropriate d-dimensional space, is given by

$$v_q = \frac{4\pi e^2}{\kappa q^2}, \quad d = 3, \tag{2a}$$

$$= \frac{2\pi e^2}{\kappa q}, \quad d = 2, \tag{2b}$$

$$= \frac{2e^2}{\kappa} K_0(qa), \quad d = 1, \tag{2c}$$

where κ is the background-material-dependent dielectric constant and K_0 denotes the zeroth-order modified Bessel function of the second kind. Note that in one dimension, the length scale a characterizes the lateral confinement size (say, radius of the 1D ribbon) and $v_q \approx -2e^2 \ln(qa)/\kappa$ for $qa \ll 1$, while $v_q = e^2/(\kappa q^2 a^2)$ for $qa \gg 1$.

The polarization function for the massive Dirac material is given by

$$\Pi(q,\omega) = \frac{g_s g_v}{L^d} \sum_{\mathbf{k},\lambda,\lambda'} F_{\lambda,\lambda'}(\mathbf{k},\mathbf{k}') \frac{n_{\rm F}(\lambda E_{\mathbf{k}}) - n_{\rm F}(\lambda' E_{\mathbf{k}'})}{\hbar\omega + \lambda E_{\mathbf{k}} - \lambda' E_{\mathbf{k}'} + i\eta}, \tag{3}$$

where $\mathbf{k}' = \mathbf{k} + \mathbf{q}$, $\lambda,\lambda' = \pm 1$ denotes the conduction (particle) and valence (hole) bands, $E_{\mathbf{k}} = \hbar v_{\rm F} |\sqrt{k^2 + (\Delta/\hbar v_{\rm F})^2}|$ with 2Δ being the energy gap, $n_{\rm F}(x)$ is the Fermi function and $2F_{\lambda,\lambda'}(\mathbf{k},\mathbf{k}') = 1 + \lambda\lambda'[\mathbf{k}\cdot\mathbf{k}' + \tilde{\Delta}^2]/(\tilde{E}_{\mathbf{k}}\tilde{E}_{\mathbf{k}'})$ is the overlap function, with $\tilde{x} \equiv x/\hbar v_{\rm F}$. The factor $g_s(=2)$ is the spin degeneracy factor and g_v is the valley (or pseudospin) degeneracy factor (e.g., $g_v = 2$ for graphene and other Dirac materials with honeycomb lattice structure). Given the general relation $\Pi(q,-\omega) = \Pi(q,\omega)^*$ and the fact that the polarization function depends only on the absolute value of the Fermi energy $\varepsilon_{\rm F}$, we only present the results for $\varepsilon_{\rm F} > 0$ and $\omega > 0$. Furthermore, we work at zero temperature so that the Fermi functions can be replaced by Heaviside step functions, i.e., $n_{\rm F}(x) = \Theta(\varepsilon_{\rm F} - x)$.

Depending upon the placement of the Fermi energy $\varepsilon_{\rm F}$, we can split our polarization function into two parts, namely, the intrinsic ($\varepsilon_{\rm F} < \Delta$) and extrinsic ($\varepsilon_{\rm F} > \Delta$) polarization:

$$\Pi(q,\omega) = -\chi_\infty^-(q,\omega) + \underbrace{\chi_{\varepsilon_{\rm F}}^-(q,\omega) + \chi_{\varepsilon_{\rm F}}^+(q,\omega)}$$

$$= \Pi_0(q,\omega) + \theta(\varepsilon_{\rm F} - \Delta)\Pi_1(q,\omega), \tag{4}$$

where

$$\chi_D^{\pm}(q,\omega) = -\frac{g_s g_v}{(2\pi)^d} \int d^d k \Theta(D^2 - \Delta^2 - k^2) \times \left(1 \pm \frac{\mathbf{k}\cdot\mathbf{k}' + \tilde{\Delta}^2}{\tilde{E}_{\mathbf{k}}\tilde{E}_{\mathbf{k}'}}\right) \times \left[\frac{E_{\mathbf{k}} \mp E_{\mathbf{k}'}}{(\hbar\omega + i\eta)^2 - (E_{\mathbf{k}} \mp E_{\mathbf{k}'})^2}\right]. \tag{5}$$

Here the upper and lower signs correspond to intraband and interband electron-hole transitions, respectively, and the parameter D defines the integration limits via the Θ function. Since we are interested in the long-wavelength ($q \to 0$) plasmon dispersion, we evaluate Eq. (3) in the dynamical limit ($q \to 0$ first and then $\omega \to 0$) to lowest order in q^2/ω^2, just above the intraband particle-hole continuum.

We mention at the outset that we will use the superscript (p), (g), and (m) to refer to systems with parabolic, gapless (or massless) Dirac, and massive Dirac systems, respectively. Note that the electronic density for any d-dimensional system, in terms of its Fermi wave vector, is given by

$$n_d = g_s g_v \frac{\pi^{d/2} {k_{\rm F}}^d}{2^d \pi^d \Gamma(1 + d/2)}, \tag{6}$$

where $\Gamma(x)$ is the Gamma function. However, the Fermi wave vectors for parabolic, massive Dirac, and gapless Dirac systems are expressed differently in terms of the Fermi energy and are given by $k_{\rm F} = \sqrt{2m\varepsilon_{\rm F}}/\hbar$, $k_{\rm F} = \sqrt{\varepsilon_{\rm F}^2 - \Delta^2}/\hbar v_{\rm F}$, and $k_{\rm F} = \varepsilon_{\rm F}/\hbar v_{\rm F}$, respectively.

For systems with parabolic dispersion ($E_{\mathbf{k}} = \hbar^2 k^2/2m_{\rm p}$), Eq. (3) can be evaluated in the dynamical long-wavelength limit, up to leading order in q just above the particle-hole continuum, to obtain

$$\Pi^{(\rm p)}(q,\omega) \approx \frac{n_d}{m_{\rm p}} \frac{q^2}{\omega^2} + O\left(\frac{q^4}{\omega^4}\right). \tag{7}$$

For massive Dirac systems, $E_{\mathbf{k}} = \hbar v_{\rm F}\sqrt{k^2 + \tilde{\Delta}^2}$ (where $\tilde{\Delta} = \Delta/\hbar v_{\rm F}$) in all dimensions, and the dynamical long-wavelength limit of the Lindhard function, just above the particle-hole continuum, is given by

$$\Pi^{(\rm m)} \approx \frac{g_s g_v v_{\rm F}}{\hbar(2\pi)^d} \frac{\pi^{d/2}}{\Gamma(1 + d/2)} \frac{k_{\rm F}^d}{\sqrt{k_{\rm F}^2 + \tilde{\Delta}^2}} \frac{q^2}{\omega^2} + O\left(\frac{q^4}{\omega^4}\right). \tag{8}$$

For massless Dirac systems such as graphene, $\Delta \to 0$ and $E_{\mathbf{k}} = \hbar v_{\rm F} k$ in all dimensions, and Eq. (8) reduces to

$$\Pi^{(\rm g)}(q,\omega) \approx \frac{g_s g_v v_{\rm F} k_{\rm F}^{d-1}}{\hbar(2\pi)^d} \frac{\pi^{d/2}}{\Gamma(1 + d/2)} \frac{q^2}{\omega^2} + O\left(\frac{q^4}{\omega^4}\right), \tag{9}$$

which is consistent with Eq. (6) of Ref. [18]. We emphasize here that even though the density dependence of the long-wavelength limit of the polarization function for massless and massive Dirac systems is different from that of the parabolic systems, they can be rewritten in the same form as Eq. (3),

$$\Pi^{(\rm m,g)}(q,\omega) \approx \frac{n_d}{\varepsilon_{\rm F}/v_F^2} \frac{q^2}{\omega^2} + O\left(\frac{q^4}{\omega^4}\right). \tag{10}$$

Note the similarity between Eqs. (7) and (10). This prompts the following mapping: band mass in parabolic systems, $m_{\rm p} \to m_{\rm d} \equiv \varepsilon_{\rm F}/v_{\rm F}^2$, density-dependent effective Dirac mass in massive as well as massless Dirac systems (to be distinguished from the band gap Δ, which is occasionally also referred to as mass). As a natural consequence, this correspondence manifests itself in all of the subsequent calculations.

Physically, the Dirac mass is a dynamical collective mass and is essential to explain inertial acceleration of the Dirac plasma under application of an external electric field. In fact, it has been insightfully defined as "plasmon mass" in the context of graphene [19], and has also been recently measured in graphene [10]. Note that $m_{\rm d} = \varepsilon_{\rm F}/v_{\rm F}^2$ is also the cyclotron effective mass ($m_{\rm c}$) for Dirac systems [35], which is typically defined as $2\pi m_c = \hbar^2 dS(\varepsilon)/d\varepsilon$, where

$S(\varepsilon) = \pi(\varepsilon^2 - \Delta^2)/\hbar^2 v_F^2$ denotes the area of a closed cyclotron orbit of massive Dirac electrons with energy ε. For a system with a parabolic dispersion, the band mass, plasmon mass, and cyclotron mass are identical, $m_p = m_c$.

Having obtained the long-wavelength limit of the dynamical polarization function, we now proceed to calculate the long-wavelength limit of the plasmon dispersion in the next section.

III. PLASMON DISPERSION

Using Eqs. (7) and (2) in Eq. (1), the well-known long-wavelength plasmon dispersion for systems with parabolic dispersion [2,5], in one, two, and three dimensions, can be easily obtained to be

$$\omega_1^{(p)} = \sqrt{\frac{2e^2 n_1}{\kappa m_p}} q\sqrt{|\ln(qa)|} + O(q^3), \tag{11a}$$

$$\omega_2^{(p)} = \sqrt{\frac{2\pi e^2 n_2}{\kappa m_p}} q^{1/2} + O(q^{3/2}), \tag{11b}$$

$$\omega_3^{(p)} = \sqrt{\frac{4\pi e^2 n_3}{\kappa m_p}} + O(q^2). \tag{11c}$$

An important point to note here is that for the first term in Eq. (11), we can substitute $m_p \to m$, i.e., replace the effective band mass by the classical mass of the particle, and the quantum mechanical plasmon dispersion takes precisely the same form as that of classical density oscillations in an electron liquid [1,2,5]. Physically, this is a direct consequence of the fact that the long-wavelength plasmons involve the motion of the entire plasma, and to lowest order it does not depend on the complex exchange and correlation effects that dress the motion of an individual electron. It should be emphasized that no such classical analog exists for Dirac systems and the plasmon dispersion in Dirac systems is intrinsically quantum mechanical in nature [18]. Note, however, that the higher-order correction terms in Eq. (11) are fully quantum mechanical and $\hbar$ explicitly appears in them.

For systems with massive Dirac dispersion, using Eqs. (8) and (2) in Eq. (1), the $q \to 0$ limit of the plasmon dispersion is given by

$$\omega_1^{(m)} = \sqrt{\frac{2ge^2 v_F}{\hbar\kappa\pi}} q\sqrt{K_0(qa)} \frac{\left(\varepsilon_F^2 - \Delta^2\right)^{1/4}}{\varepsilon_F^{1/2}} + O(q^3), \tag{12a}$$

$$\omega_2^{(m)} = \sqrt{\frac{ge^2}{2\kappa\hbar^2}} \sqrt{\frac{\varepsilon_F^2 - \Delta^2}{\varepsilon_F}} q^{1/2} + O(q^{3/2}), \tag{12b}$$

$$\omega_3^{(m)} = \sqrt{\frac{2ge^2}{3\pi\kappa\hbar^3 v_F}} \frac{\left(\varepsilon_F^2 - \Delta^2\right)^{3/4}}{\varepsilon_F^{1/2}} + O(q^2), \tag{12c}$$

where we have defined $g \equiv g_s g_v$. Note that 2D massive Dirac plasma was also studied in Ref. [24], which reported an expression similar to Eq. (12b). For the limiting case of $\Delta \to 0$, Eq. (12) leads to

$$\omega_1^{(g)} = \sqrt{\frac{2ge^2 v_F}{\hbar\kappa\pi}} q\sqrt{K_0(qa)} + O(q^3), \tag{13a}$$

$$\omega_2^{(g)} = \sqrt{\frac{ge^2\varepsilon_F}{2\kappa\hbar^2}} q^{1/2} + O(q^{3/2}), \tag{13b}$$

$$\omega_3^{(g)} = \sqrt{\frac{2ge^2\varepsilon_F^2}{3\pi\kappa\hbar^3 v_F}} + O(q^2). \tag{13c}$$

Equation (13) reproduces the results for the gapless Dirac plasma reported in Ref. [18]. One important similarity between Eqs. (11)–(13) is the same functional dependence of the plasmon frequency on the wave vector q. This is a direct consequence of the physical requirement that the long-wavelength plasmon dispersion must satisfy particle conservation (or continuity equation). One important difference between parabolic and Dirac systems is that while the long-wavelength limit of plasmon dispersion in parabolic systems is essentially "classical" in nature, the plasmon dispersion in GDP and MDP is essentially quantum mechanical, as evidenced by the explicit appearance of $\hbar$ in Eqs. (12) and (13).

The long-wavelength dependence of the dynamical polarization function is the same for parabolic systems, GDP, and MDP: $\Pi \propto q^2/\omega^2$; however, the proportionality constant has a different density dependence for various systems. For parabolic systems, $\Pi^{(p)} \propto n_d$, for gapless Dirac systems, $\Pi^{(g)} \propto n_d^{1-1/d}$, and for massive Dirac systems, $\Pi^{(m)} \propto n_d/(n_d^{2/d} + \alpha_d\tilde{\Delta}^2)^{1/2}$, where $\alpha_d = (g/\pi)^2, g/4\pi, (g/6\pi^2)^{2/3}$ in one, two, and three dimensions, respectively. As a consequence, the density dependence of the long-wavelength plasmon frequency for MDP is completely different compared to GDP and parabolic dispersion systems. As seen from Eq. (11), the plasmon frequency for a parabolic dispersion system is proportional to $\sqrt{n_d}$ in all dimensions. However, for GDP, the plasmon dispersion follows $\omega_d^{(g)} \propto \sqrt{n_d}/n_d^{1/2d}$ behavior, and for the one-dimensional case, the plasmon mode is completely independent of the density. For the MDP case, the density dependence completely changes due to the presence of gap and takes the form $\omega_d^{(m)} \propto \sqrt{n_d}/(n_d^{2/d} + \alpha_d\tilde{\Delta}^2)^{1/4}$, where $\alpha_d = (g/\pi)^2, g/4\pi, (g/6\pi^2)^{2/3}$, in one, two, and three dimensions, respectively. Note that in one dimension, the plasmon frequency in GDP is independent of the density, whereas for MDP the plasmon frequency of MDP has an explicit dependence on n_1, as evident from Eq. (12a).

Similar to the case of the long-wavelength polarization function in Eq. (10), the plasmon frequencies in the $q \to 0$ limit in GDP and MDP can also be rewritten in the form similar to Eq. (11) for parabolic systems,

$$\omega_1^{(m,g)} = \sqrt{\frac{2e^2 n_1}{\kappa m_d}} q\sqrt{K_0(qa)} + O(q^3), \tag{14a}$$

$$\omega_2^{(m,g)} = \sqrt{\frac{2\pi e^2 n_2}{\kappa m_d}} q^{1/2} + O(q^{3/2}), \tag{14b}$$

$$\omega_3^{(m,g)} = \sqrt{\frac{4\pi e^2 n_3}{\kappa m_d}} + O(q^2). \tag{14c}$$

We emphasize again that even though the density dependence of plasmon frequencies in the long-wavelength limit in the GDP and MDP is different from that of the parabolic systems, the frequencies can be rewritten in the same form using the density-dependent effective Dirac mass (or, equivalently, the cyclotron mass). However, we note that this simplicity is deceptive, since for parabolic systems the band mass $m_{\rm p}$ and density n_d can also be treated as classical independent variables, but for Dirac systems $m_{\rm d}$ is density dependent via the Fermi energy in a purely quantum mechanical way.

IV. PLASMONS IN METAMATERIALS MADE OF MASSIVE DIRAC PLASMA, RIBBON, AND LAYER ARRAYS

In this section, we consider collective density excitations in metamaterials (periodic arrays) of massive Dirac plasma systems. In particular, we consider a stacking of identical 1D massive Dirac plasma nanoribbons (or quantum wires) placed parallel to each other in a plane, and a periodic array of parallel 2D massive Dirac plasma sheets. Similar systems made of parabolic dispersion and gapless Dirac plasma have been theoretically investigated earlier [18,28–30,33] and experimentally demonstrated for graphene [8,9,11]. To describe the collective modes of such superstructures, we need to include the inter-ribbon or interlayer Coulomb interactions, which leads to a coupling of all the layers due to the long-range nature of Coulomb interactions. Assuming no wave-function overlap between any consecutive layers or nanoribbons, the collective modes of such superlattices, within RPA, are given by the zeros of the determinant of the general dielectric matrix of the superlattice, whose elements are given by

$$\epsilon_{ll'} = \delta_{ll'} - v_{ll'}(q,k)\Pi_{l'}(q,\omega), \tag{15}$$

where $\Pi_l(q,\omega) = \Pi(q,\omega)$ is the bare density-density response function of each nanoribbon or layer whose long-wavelength limit is given in Eq. (8). In Eq. (15), $v_{ll'}(q,k)$ is the repulsive Coulomb interaction between the l and l' nanoribbon or layer in the periodic array which is given by

$$v_{ll'} = \frac{2\pi e^2}{\kappa q} e^{-qb|l-l'|}, \quad d = 2, \tag{16a}$$

$$v_{ll'} = \frac{2e^2}{\kappa}[\delta_{ll'}K_0(qa) + (1-\delta_{ll'})K_0(qb|l-l'|)], \quad d = 1, \tag{16b}$$

where b is the superlattice spacing.

Assuming a periodic boundary conditions for the 1D superlattice, the eigenvalues of the general dielectric matrix in Eq. (15) are given by $1 - v_q\Pi(q,\omega)S_d(q,k)$, where $S_d(q,k) = v_q^{-1}\sum_{l'} v_{ll'}e^{-ik(l-l')b}$ is the form factor for the 1D superlattice formed from a d-dimensional plasma, and k is to be interpreted as a new wave vector arising from the periodicity of the infinite superlattice array and $|k| < \pi/b$. For definiteness, we take the 1D MDP wire array to be along the x axis ($q = q_x$) and $k = q_y$ to be along the superlattice direction of the y axis. For the 2D MDP layer superlattice, we consider it to lie in the $x-y$ plane and the wave vector $k = q_z$ to be along the superlattice direction—the z axis. The dimensionless form factors can now be evaluated and are given by

$$S_1 = 1 + \frac{2}{K_0(qa)}\sum_{n=1}^{\infty} K_0(nqb)\cos(nq_y b), \tag{17a}$$

$$S_2 = \sum_{n=-\infty}^{\infty} e^{-q|n|b - iq_z nb} = \frac{\sinh(qb)}{\cosh(qb) - \cos(q_z b)}. \tag{17b}$$

Note that for $q_z = 0$, as $q \to 0$, $S_2 \to q$. The plasmon bands for the 1D superlattice, i.e., $\omega_{ds}^{(p,m,g)}$ composed of Schrödinger electrons, MDP, and GDP, are now explicitly given by the zeros of the eigenvalues of the general dielectric matrix in Eq. (15),

$$1 - v_q\Pi(q,\omega)S_d(q,k) = 0. \tag{18}$$

However, in the long-wavelength dynamical limit ($q \to 0$), $\Pi \propto q^2/\omega^2$ for parabolic, massive Dirac, and gapless Dirac systems in all dimensions and, consequently, Eq. (18) simplifies to give

$$\omega_{ds}^{(p,m,g)} = \omega_d^{(p,m,g)} S_d^{1/2}, \tag{19}$$

where the form factor S_d is explicitly given in Eq. (17). We emphasize that Eq. (19) is very general and it describes the long-wavelength plasmon dispersion for a 1D superlattice made of parabolic, massive Dirac, or gapless Dirac systems (for both ribbons and layers). The plasmon bands for a superlattice of 1D MDP nanoribbons and 2D MDP layers is displayed in Figs. 1(a) and 1(b), respectively, against the backdrop of the particle-hole continuum.

For ribbons and layers of parabolic systems, the superlattice plasmon dispersion at the upper band edge ($k = 0$) is given by

$$\omega_{1s}^{(p)}(q; q_y = 0) = \left(\frac{2\pi\tilde{n}_2 e^2 q}{\kappa m_{\rm p}}\right)^{1/2}, \tag{20a}$$

$$\omega_{2s}^{(p)}(q; q_z = 0) = \left(\frac{4\pi\tilde{n}_3 e^2}{\kappa m_{\rm p}}\right)^{1/2}, \tag{20b}$$

with $\tilde{n}_2 = \frac{n_1}{b}$ and $\tilde{n}_3 = \frac{n_2}{b}$. Note that in Eq. (20), the d-dimensional superlattice plasmon at the band edge ($k = 0$) has exactly the same form as the corresponding $(d+1)$-dimensional bulk plasmon [see Eqs. (11a) and (11b)] with the effective densities being $\tilde{n}_3 = n_2/b$ and $\tilde{n}_2 = n_1/b$. This is consistent physically since the d-dimensional superlattice loses its discrete periodicity at the band edge ($k = 0$) and effectively becomes a $(d+1)$-dimensional system.

In the case of superlattice structures made of MDP, the $q \to 0$ plasmon dispersion at the band edge ($k = 0$) is

$$\omega_{1s}^{(m)}(q; q_y = 0) = \sqrt{\frac{2ge^2 v_{\rm F} q}{\hbar\kappa b}}\frac{\left(\varepsilon_{\rm F}^2 - \Delta^2\right)^{1/4}}{\varepsilon_{\rm F}^{1/2}}, \tag{21a}$$

$$\omega_{2s}^{(m)}(q; q_z = 0) = \sqrt{\frac{ge^2}{\hbar^2\kappa b}}\sqrt{\frac{\varepsilon_{\rm F}^2 - \Delta^2}{\varepsilon_{\rm F}}}. \tag{21b}$$

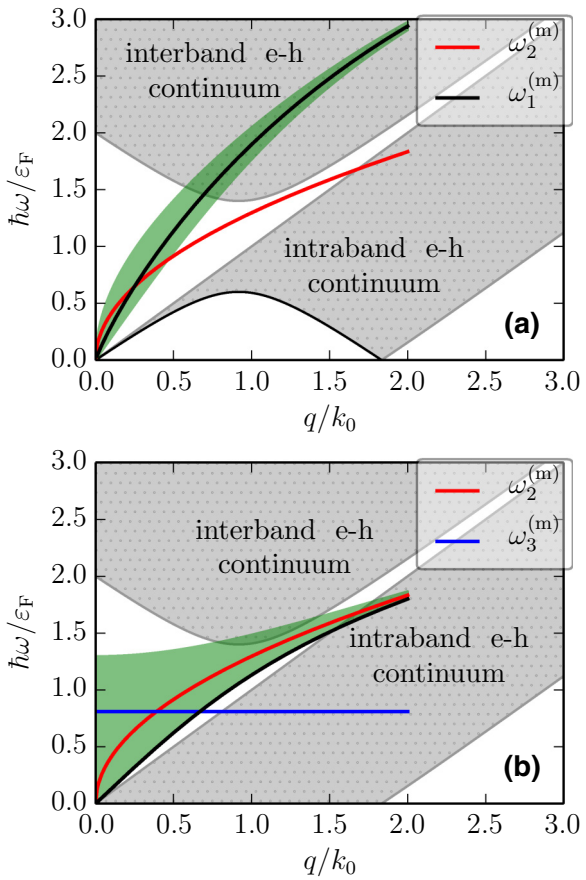

FIG. 1. (Color online) (a) The long-wavelength plasmon dispersion for 1D and 2D MDP against the backdrop of the 1D particle-hole continuum (the gray shaded region). The green shaded region marks the plasmon band formed in the 1D superlattice of the 1D MDP [the lower boundary is for $q_y = \pi/b$ and the upper boundary is for $q_y = 0$ in Eq. (19)]. (b) The long-wavelength plasmon dispersion for 2D and 3D MDP, with the green shaded region marking the plasmon band formed in the 1D superlattice of the 2D MDP (the lower boundary is for $q_z = \pi/b$ and the upper boundary is for $q_z = 0$). The gray shaded region in (b) depicts the particle-hole continuum of 2D and 3D massive plasma. Note that as in the parabolic case, the electron-hole continuum in 1D differs from the 2D and 3D case because there are no excitations at finite q and low ω even for massive and massless Dirac fermions. In both panels, we have defined $\hbar v_F k_0 \equiv \varepsilon_F$ and used the following parameters: $\Delta/\varepsilon_F = 0.4$, $ge^2/(2\hbar\kappa v_F) = 2$, $ak_0 = 0.25$, and $bk_0 = 2$.

These, in the limit $\Delta \to 0$, give the corresponding expressions for the GDP:

$$\omega_{1s}^{(g)}(q;q_y=0) = \left(\frac{2ge^2 v_F q}{\hbar\kappa b}\right)^{1/2}, \tag{22a}$$

$$\omega_{2s}^{(g)}(q;q_z=0) = \left(\frac{e^2 g\varepsilon_F}{\hbar^2\kappa b}\right)^{1/2}. \tag{22b}$$

The physically appealing correspondence between the d-dimensional superlattice at the band edge and $(d+1)$-dimensional bulk system does not happen for MDP as well as for GDP. From Eqs. (21a) and (21b), it is clear that at the band edge, $\omega_{1s}^{(m,g)}(q;q_y=0) \neq \omega_2^{(m,g)}$ with the intuitive substitution $\tilde{n}_2 = n_1/b$ and $\omega_{2s}^{(m,g)}(q;q_z=0) \neq \omega_3^{(m,g)}$ with $\tilde{n}_3 = n_2/b$. This is a direct consequence of different density dependence of the polarization function [see Eqs. (8) and (9)] in massive and massless Dirac systems as compared to systems with a parabolic dispersion relation [see Eq. (7)]. However, the 2D superlattice plasmon dispersion would map to the corresponding plasmon dispersion for 3D massive Dirac plasma $\omega_{2s}^{(m)}(q;q_z=0,n_2) \to \omega_3^{(m)}(q,\tilde{n}_3)$ if, rather than the intuitive definition $\tilde{n}_3 = n_2/b$, we have the following correspondence of densities in 3D and 2D massive systems:

$$\left(\frac{\tilde{n}_3 b}{n_2}\right)^2 = \frac{(6\pi^2\tilde{n}_3 g^{-1})^{2/3} + \tilde{\Delta}^2}{4\pi n_2 g^{-1} + \tilde{\Delta}^2}. \tag{23}$$

In the $\Delta \to 0$ limit, Eq. (23) leads to the corresponding relation GDP, i.e., $\tilde{n}_3 = (9\pi g/16)^{1/4}(n_2/b^2)^{3/4}$, which was first derived in Ref. [18]. For the 1D superlattice, the gapless Dirac plasma frequency $\omega_{1s}^{(g)}$ does not depend on the carrier density at all, and hence massive Dirac plasma frequency differs here in this aspect. For 1D massive Dirac plasma, the superlattice plasmon frequency at the band edge would agree with the 2D massive plasma frequency, i.e., $\omega_{1s}^{(m)}(q;q_y=0,n_1) \to \omega_2^{(m)}(q,\tilde{n}_2)$, only if we have the following relation between the densities $\tilde{n}_2$ and n_1:

$$\left(\frac{\tilde{n}_2 b}{n_1}\right)^2 = \frac{4\pi\tilde{n}_2 g + g^2\tilde{\Delta}^2}{\pi^2 n_1^2 + g^2\tilde{\Delta}^2}. \tag{24}$$

In the $\Delta \to 0$ limit, Eq. (24) reproduces the corresponding relation GDP, i.e., $\tilde{n}_2 = 4g/\pi b^2$.

Due to the presence of gap in massive Dirac systems, the density dependence as well as the band-edge plasmon at $k = 0$ differs from the usual parabolic as well as the massless Dirac systems. This is because of the fact that the density dependence of the polarizability of massive Dirac systems is completely different compared to massless Dirac and parabolic dispersion systems, as shown in Eqs. (8).

Finally, we note that as in the case of bulk plasmons, in Eqs. (14a)–(14c), the superlattice plasmon frequencies for Dirac systems can be expressed in the same form as for systems with parabolic dispersion relation. Expressing the numerator in Eqs. (21a)–(25a) in terms of density and the denominator in terms of the cyclotron mass of massive Dirac particles $m_d = \varepsilon_F/v_F^2$, we have

$$\omega_{1s}^{(m,g)}(q;q_y=0) = \left(\frac{2\pi\tilde{n}_2 e^2 q}{\kappa m_d}\right)^{1/2}, \tag{25a}$$

$$\omega_{2s}^{(m,g)}(q;q_z=0) = \left(\frac{4\pi\tilde{n}_3 e^2}{\kappa m_d}\right)^{1/2}. \tag{25b}$$

V. SUMMARY AND CONCLUSION

In this paper, we have obtained the long-wavelength plasmon frequency for massive Dirac particles in various dimensions and their 1D superlattice, and compared it with the corresponding results for plasmons in parabolic systems and gapless Dirac systems. As expected, factors of $1/\sqrt{\hbar}$ explicitly appear even in the leading-order term in the long-wavelength plasmon dispersion of MDP and GDP, highlighting their intrinsically nonclassical and quantum nature.

To summarize, we find that the long-wavelength limit of the dynamical density response function, while having the same

dependence for q and ω, i.e., $\Pi \propto q^2/\omega^2$ for parabolic as well as Dirac systems, has a different dependence on density. This different density dependence also gets manifested in the long-wavelength plasmon dispersion and we find that for massive Dirac systems, $\omega_d^{(\mathrm{m})} \propto \sqrt{n_d}/(n_d^{2/d} + \alpha_d \tilde{\Delta}^2)^{1/4}$, while for gapless Dirac systems, $\omega^{(\mathrm{g})} \propto \sqrt{n_d}/n_d^{1/2d}$, and for parabolic systems, $\omega^{(\mathrm{p})} \propto \sqrt{n_d}$, in d-dimensional systems. Additionally, we note that a beautiful similarity emerges between all three systems if we use the density-dependent effective Dirac mass (or cyclotron mass) for GDP and MDP, $m_{\mathrm{d}} = \varepsilon_{\mathrm{F}}/v_{\mathrm{F}}^2$, to express the long-wavelength plasmon dispersion for all systems in all dimensions: $\omega^{(\mathrm{p,g,m})} \propto \sqrt{n_d/m_{\mathrm{p/d}}}$. This density dependence of the plasmon frequency may be used to distinguish between various types of systems (parabolic, GDP, and MDP) and their effective dimensionality. Alternatively, the long-wavelength plasmon dispersion may be used to determine the dynamical collective mass of various Dirac systems [10].

We have also calculated the plasmon dispersion in a 1D superlattice made of nanoribbons and layers of MDP, and find that while the q dependence is similar to that of parabolic superlattice, the density dependence is completely different. Note that our results for the 3D plasmons of MDP, 2D layers, and multilayers, as well as 1D ribbons and multiribbon arrays can be tested using electron scattering, light scattering, or infrared spectroscopy for ribbons and layers made of silicene, transition-metal dichalcogenides, and other materials which have a dispersion similar to that of massive or gapped Dirac spectrum at low energies.

Finally, we note that we have not included in our calculation the effect of dielectric mismatch, which may lead to the dielectric constant appearing in the expression of the Coulomb interaction κ to be wave-vector dependent. This can be easily included in our calculations according to Ref. [36]. However, we believe that the long-wavelength plasmon dispersion, as discussed in this paper, would not be impacted by this, even though the dielectric mismatch may change the plasmon dispersion for finite wave vectors.

ACKNOWLEDGMENTS

We gratefully acknowledge funding from the INSPIRE Faculty Award by DST (Government of India) (A.A.) and from the Faculty Initiation Grant by IIT Kanpur, India (A.A.). We also acknowledge financial support by NSF Grant No. DMR-1406568 (G.V.).

[1] D. Pines and P. Noziéres, *The Theory of Quantum Liquids* (W. A. Benjamin, New York, 1966).
[2] G. F. Giuliani and G. Vignale, *Quantum Theory of the Electron Liquid* (Cambridge University Press, Cambridge, 2005).
[3] S. A. Maier, *Plasmonics: Fundamentals and Applications* (Springer, New York, 2007).
[4] M. S. Tame, K. R. McEnery, S. K. Özdemir, J. Lee, S. A. Maier, and M. S. Kim, Nat. Phys. **9**, 329 (2013).
[5] T. Ando, A. B. Fowler, and F. Stern, Rev. Mod. Phys. **54**, 437 (1982).
[6] A. Agarwal, S. Chesi, T. Jungwirth, J. Sinova, G. Vignale, and M. Polini, Phys. Rev. B **83**, 115135 (2011); A. Agarwal, M. Polini, R. Fazio, and G. Vignale, Phys. Rev. Lett. **107**, 077004 (2011).
[7] A. Agarwal, M. Polini, G. Vignale, and M. E. Flatté, Phys. Rev. B **90**, 155409 (2014).
[8] L. Ju, B. Geng, J. Horng, C. Girit, M. Martin, Z. Hao, H. A. Bechtel, X. Liang, A. Zettl, Y. Ron Shen, and F. Wang, Nat. Nanotechnol. **6**, 630 (2011).
[9] H. Yan, X. Li, B. Chandra, G. Tulevski, Y. Wu, M. Freitag, W. Zhu, P. Avouris, and F. Xia, Nat. Nanotechnol. **7**, 330 (2012).
[10] H. Yoon, C. Forsythe, L. Wang, N. Tombros, K. Watanabe, T. Taniguchi, J. Hone, P. Kimand, and D. Ham, Nat. Nanotechnol. **9**, 594 (2014).
[11] H. Yan, T. Low, W. Zhu, Y. Wu, M. Freitag, X. Li, F. Guinea, P. Avourisand, and F. Xia, Nat. Photon. **7**, 394 (2013).
[12] A. N. Grigorenko, M. Polini, and K. S. Novoselov, Nat. Photon. **6**, 749 (2012).
[13] T. Stauber, J. Phys.: Condens. Matter **26**, 123201 (2014).
[14] Z. Fei *et al.*, Nano Lett. **11**, 4701 (2011).
[15] B. Wunsch, T. Stauber, F. Sols, and F. Guinea, New J. Phys. **8**, 318 (2006).
[16] E. H. Hwang and S. Das Sarma, Phys. Rev. B **75**, 205418 (2007).
[17] M. Polini, R. Asgari, G. Borghi, Y. Barlas, T. Pereg-Barnea, and A. H. MacDonald, Phys. Rev. B **77**, 081411(R) (2008).
[18] S. Das Sarma and E. H. Hwang, Phys. Rev. Lett. **102**, 206412 (2009).
[19] S. H. Abedinpour, G. Vignale, A. Principi, M. Polini, W. K. Tse, and A. H. MacDonald, Phys. Rev. B **84**, 045429 (2011).
[20] P. Di Pietro, M. Ortolani, O. Limaj, A. Di Gaspare, V. Giliberti, F. Giorgianni, M. Brahlek, N. Bansal, N. Koirala, S. Oh, P. Calvani, and S. Lupi, Nat. Nano **8**, 556 (2013).
[21] S. Raghu, S. B. Chung, X.-L. Qi, and S.-C. Zhang, Phys. Rev. Lett. **104**, 116401 (2010).
[22] M. Lv and S.-C. Zhang, Int. J. Mod. Phys. B **27**, 1350177 (2013).
[23] J. Zhou, H.-R. Chang, and D. Xiao, Phys. Rev. B **91**, 035114 (2015).
[24] P. K. Pyatkovskiy, J. Phys.: Condens. Matter **21**, 025506 (2009).
[25] C. J. Tabert and E. J. Nicol, Phys. Rev. B **89**, 195410 (2014).
[26] H. R. Chang, J. Zhou, H. Zhang, and Y. Yao, Phys. Rev. B **89**, 201411(R) (2014).
[27] B. Van Duppen, P. Vasilopoulos, and F. M. Peeters, Phys. Rev. B **90**, 035142 (2014).
[28] S. Das Sarma and J. J. Quinn, Phys. Rev. B **25**, 7603 (1982).
[29] S. Das Sarma and Wu-yan Lai, Phys. Rev. B **32**, 1401(R) (1985).
[30] T. Low, R. Roldan, H. Wang, F. Xia, P. Avouris, L. M. Moreno, and F. Guinea, Phys. Rev. Lett. **113**, 106802 (2014).
[31] A. S. Rodin and A. H. Castro Neto, Phys. Rev. B **91**, 075422 (2015).
[32] E. H. Hwang and S. Das Sarma, Phys. Rev. B **80**, 205405 (2009).
[33] J.-J. Zhu, S. M. Badalyan, and F. M. Peeters, Phys. Rev. B **87**, 085401 (2013).
[34] C. Triola and E. Rossi, Phys. Rev. B **86**, 161408(R) (2012).
[35] A. R. Wright and R. H. McKenzie, Phys. Rev. B **87**, 085411 (2013).
[36] S. M. Badalyan and F. M. Peeters, Phys. Rev. B **85**, 195444 (2012).